AIP | Applied Physics Letters

Plasmon-polaritons on graphene-metal surface and their use in biosensors

Omer Salihoglu, Sinan Balci, and Coskun Kocabas

Citation: Applied Physics Letters **100**, 213110 (2012); doi: 10.1063/1.4721453
View online: http://dx.doi.org/10.1063/1.4721453
View Table of Contents: http://scitation.aip.org/content/aip/journal/apl/100/21?ver=pdfcov
Published by the AIP Publishing

Articles you may be interested in

Extremely confined terahertz surface plasmon-polaritons in graphene-metal structures
Appl. Phys. Lett. **103**, 071103 (2013); 10.1063/1.4818660

Development of a surface plasmon resonance and nanomechanical biosensing hybrid platform for multiparametric reading
Rev. Sci. Instrum. **84**, 015008 (2013); 10.1063/1.4789430

Probing molecular interactions on carbon nanotube surfaces using surface plasmon resonance sensors
Appl. Phys. Lett. **101**, 223114 (2012); 10.1063/1.4768927

Thiolene-based microfluidic flow cells for surface plasmon resonance imaging
Biomicrofluidics **5**, 026501 (2011); 10.1063/1.3596395

Spectral sensitivity of two-dimensional nanohole array surface plasmon polariton resonance sensor
Appl. Phys. Lett. **91**, 123112 (2007); 10.1063/1.2789181

AIP | Journal of Applied Physics



Journal of Applied Physics is pleased to announce André Anders as its new Editor-in-Chief

This article is copyrighted as indicated in the article. Reuse of AIP content is subject to the terms at: http://scitation.aip.org/termsconditions. Downloaded to IP: 139.179.2.116 On: Tue, 15 Jul 2014 06:31:48

Plasmon-polaritons on graphene-metal surface and their use in biosensors

Omer Salihoglu,[1] Sinan Balci,[2] and Coskun Kocabas[1,a)]
[1]*Department of Physics, Bilkent University, 06800 Ankara, Turkey*
[2]*Department of Mechanical Engineering, University of Turkish Aeronautical Association, 06790 Ankara, Turkey*

(Received 26 March 2012; accepted 6 May 2012; published online 23 May 2012)

We studied excitation of surface plasmon-polaritons on graphene-metal surface. The metal surface is functionalized by transfer printing of graphene grown by chemical vapor deposition on copper foils. Surface plasmon resonance characteristics of monolayer and multilayer graphene on the metal surface are presented. We were able to obtain the dispersion relation of graphene-metal surface which reveals the essential feature of the plasmon-polaritons. As an application, we fabricated a surface plasmon resonance sensor integrated with a microfluidic device to study nonspecific physical interaction between graphene layer and proteins. © *2012 American Institute of Physics*. [http://dx.doi.org/10.1063/1.4721453]

The unique electronic band structure of the two-dimensional crystal of carbon, graphene stimulated a great research interest in the past few years.[1] The Dirac electrons of graphene provide a linear dispersion with very small effective mass. These unusual electronic properties of graphene together with the ability to be synthesized over large area make graphene a promising material especially for fast electronic circuits.[2–6] The lack of the band gap limits the application of graphene in digital electronics while some analog electronic applications are still possible.[3,5,7] Although the main research focus is concentrated on the conventional electronics, many unusual applications of graphene emerge. Graphene based macroelectronics,[8] photonics,[9,10] and optoelectronics[11,12] are promising research areas where unusual properties of graphene can provide new perspectives.

Plasmonics[13–15] is another interesting field of research for rising applications of graphene. We anticipate that graphene can provide new perspectives in plasmonics in three different ways: (1) as a surface which directly supports surface plasmons at infrared frequencies,[14,16,17] (2) as a tunable transparent platform whose optical properties can be tuned by an external electric field,[18–20] and (3) as a functional coating for the existing plasmonic devices.[21–26]

In this paper, we demonstrate an application of graphene in plasmonics as an example for a functional coating. The primary goal of the paper is to understand the plasmonic properties of graphene coated metal surfaces. We studied the excitation of surface plasmon-polaritons (SPP) on graphene-metal surface. In this study we choose 50 nm thick silver and gold films on glass substrate as a surface to support surface plasmon-polaritons. The surfaces were coated with monolayer and multilayer graphene. Dispersion curves of SPPs on graphene coated metal surfaces reveal the essential feature of the SPP. As an application, we fabricated a surface plasmon resonance sensor (SPR) that uses a graphene coated gold as a functional surface to probe adsorption of molecules on graphene layer from an aqueous solution. This type of SPR sensors have been proposed before but have not been demonstrated yet.[21,22] Particularly, we studied nonspecific adsorption of a serum albumin protein (BSA, bovine serum albumin) on a graphene layer using a microfluidic device integrated with a graphene functionalized SPR sensor.

Immobilization of ligands on SPR sensors is an essential issue for bioanalytical applications. Direct adsorption of proteins on metal surface results in denaturalization of proteins and loss of their binding activity. Extensive efforts have been made to develop proper coating to immobilized specific ligands. The surface coating has to be thin enough to prevent detrimental effects on the plasmonic properties and should allow proper surface chemistry for immobilization of specific ligands. Self-assembled monolayers,[27] dextran, and hydrogels are most commonly used surface coatings for SPR sensors. Besides being a unique platform to study adsorption on graphitic surfaces, we believe that graphene coating can also provide new advantages for bioanalytical applications. Graphene functionalized SPR sensors have three advantages, presence of graphene layer (1) increases the adsorption of organic molecules due to π-π stacking, (2) passivates the surface against oxidation,[28] and (3) minimizes the detrimental effects on plasmonic properties.

Figure 1 illustrates the transfer printing process of the graphene on metal surface. The graphene layers were synthesized on copper foils by chemical vapor deposition.[29] The copper foils were placed in a quartz chamber and heated to 1000 °C under flow of hydrogen and argon gases. In order to reduce the oxide layer, the samples were annealed for 20 min at 1000 °C. After the annealing process, methane gas with a flow rate of 15 sccm (standard cubic centimeters per minute) was sent to the chamber for 20 min. The chamber pressure was kept at 5 Torr during the growth. The growth was terminated by stopping the flow of methane gas, and then the chamber was cooled back to the room temperature. The graphene coated copper foils were spin coated with a photoresist (PR, AZ5214) with a thickness of 1.4 μm. A flat elastomeric stamp (Polydimethylsiloxane, PDMS) was placed on the PR layer and the copper foil was etched by 1 M iron chloride solution. After the etching process, the PR with graphene remains on the PDMS stamp. The stamp was applied on 50 nm metal coated glass slide and heated to 80 °C to release

a)Author to whom correspondence should be addressed. Electronic mail: ckocabas@fen.bilkent.edu.tr. Tel.: +90(312)2901965.

 © 2012 American Institute of Physics

This article is copyrighted as indicated in the article. Reuse of AIP content is subject to the terms at: http://scitation.aip.org/termsconditions. Downloaded to IP: 139.179.2.116 On: Tue, 15 Jul 2014 06:31:48

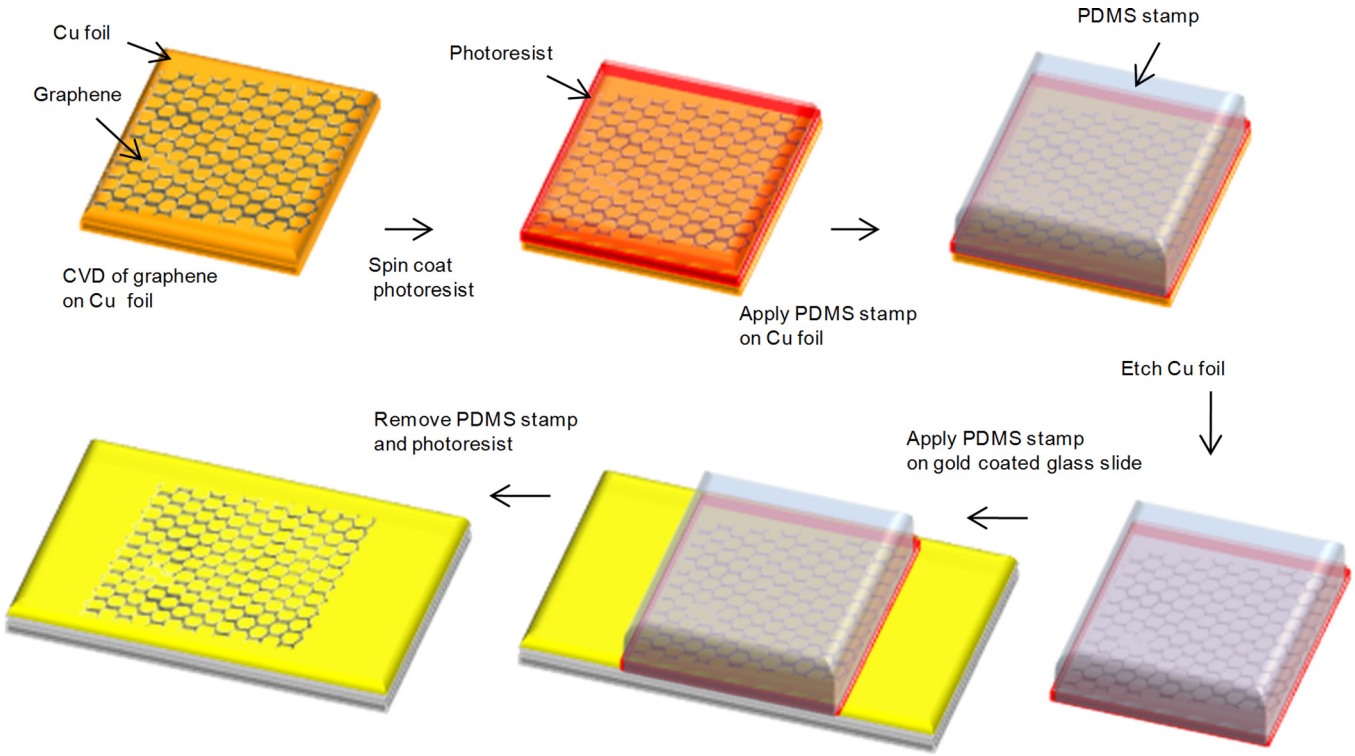


FIG. 1. Transfer printing process of graphene on a metal surface.

the PR. After removing the stamp, the PR was removed in acetone. As a result, we have large area graphene on 50 nm thick gold or silver surface. In order to obtain multilayer graphene on the metal surface, we repeated the transfer printing process. Chemical vapor deposition of graphene directly on gold and silver surfaces is also possible.[30]

The transfer printed graphene layers were characterized using Raman spectroscopy and optical absorption. Fig. 2(a) shows Raman spectra of as grown graphene on copper and transfer printed graphene on silver and gold surfaces. The G-band and 2D-band Raman signals are clearly seen from the spectra. The intensity of D-band is very small, indicating high quality graphene layer even after the transfer printing process. The intensity ratio of 2D to G band is around 1.7 and the Lorentzian linewidth of 2D band is 37 cm^{-1}. There is a slight red shift ($\sim$43 cm^{-1}) in the frequency of 2D peak after the transfer process likely because of release of the stress on the graphene. Repeating the transfer process, we obtained multilayer graphene coating. We do not observe any significant change in the spectra for multilayer graphene indicating that the graphene layers are not interacting.[31] Furthermore, we obtained the optical transmission spectra of the multilayer films on a transparent quartz substrate (see Fig. 2(b)). The transmission spectra show about 2% absorption for each graphene layer. This further supports the transfer process of single layer graphene. The area of transferred graphene layers is around 1cm^2.

After transfer printing of each graphene layer, we characterized the resonance condition for excitation of surface plasmon-polaritons on the graphene functionalized metal surface. Fig. 2(c) shows the schematic drawing of the experimental setup. The surface plasmon-polaritons were exited through a prism in Kretschmann configuration, which is needed to overcome the momentum mismatch between the excitation source and SPPs. A supercontinuum laser (Koheras-SuperK Versa) with an acousto-optic tunable filter was used as a tunable light source with a spectral width of 1 nm. The incidence angle was controlled with a motorized rotary stage with an accuracy of 0.01°. The polarization dependent reflection from the metal surface is detected with a photodiode (Newport 818) connected to an amplifier. Fig. 2(d) shows the reflectivity of the gold surface as a function of incident angle before and after transfer printing graphene. The reflection goes to minima where the phase matching condition between the incident light and surface-plasmon-polariton is satisfied. The phase matching condition is satisfied when the horizontal component of momentum of light matches the real part of momentum of SPPs. This condition can be written as

$$k_0 n_p \sin(\theta_r) = \mathrm{Re}(k_{sp}) = \mathrm{Re}\left(\frac{2\pi}{\lambda}\sqrt{\frac{\varepsilon_m \varepsilon_d}{\varepsilon_m + \varepsilon_d}}\right), \qquad (1)$$

where λ is the wavelength and k_0 is the free space wave vector of the excitation light, k_{sp} is the wavevector of surface plasmon-polaritons, n_p is the refractive index of the prism, θ_r in the resonance angle, and ε_m and ε_d are the dielectric constants of graphene coated metal surface and dielectric medium on the surface, respectively. The resonance angles for the bare gold surface and graphene functionalized gold surface are 44° and 45°, respectively. There is around 1° shift in the plasmon resonance angle.

Dispersion curve of SPP on the metal surface could provide a useful piece of information to understand the nature of

This article is copyrighted as indicated in the article. Reuse of AIP content is subject to the terms at: http://scitation.aip.org/termsconditions. Downloaded to IP: 139.179.2.116 On: Tue, 15 Jul 2014 06:31:48

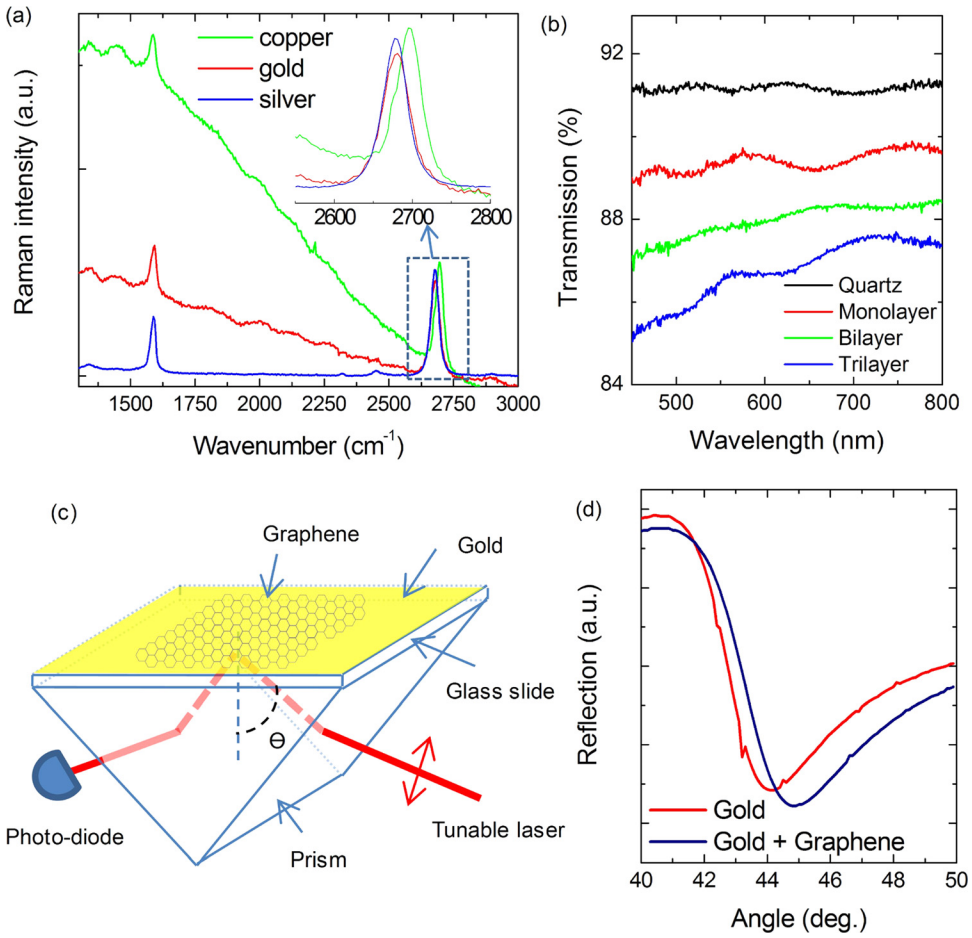


FIG. 2. (a) Raman spectra of as grown graphene on copper (green) and transfer printed graphene on silver (blue) and gold (red) surface. The intensity of the defect mode (D) is negligibly small. (b) Transmission spectra of multilayer graphene on transparent quartz substrates. Each layer has around 2% optical absorption. (c) Schematic representation of the Kretschmann configuration used to excite surface plasmon-polariton on graphene-gold surface. (d) Surface plasmon resonance curves for gold surface before (red) and after (blue) transfer printing graphene. The wavelength of the incident light is 632 nm. The presence of the graphene introduces 1° shift in the resonance angle.

the bound excitations. A standard dispersion curve provides energy-momentum relation of an excitation. Since the momentum of SPP is coupled to the incidence angle and the wavelength of the excitation (see Eq. (1)), we cannot scan momentum independently. To obtain the energy-momentum relation, we first measure angular dispersion curves (wavelength vs. incidence angle), and then calculate the energy momentum relation. The minima in the transverse magnetic (TM) polarized reflectivity maps provide the resonance condition for the excitation of SPPs. There are two resonances in the reflection spectrum. The resonance at 400–500 nm is the bulk plasmon resonance, which is independent of incidence angle and surface coating. The second resonance is the surface plasmon resonance, which has dispersion characteristics with dependence on the dielectric constant of the coating. Figure 3 provides the SPR characteristics of multilayer graphene (monolayer, bilayer, and trilayer) on metal surfaces. The multilayer graphene is obtained by sequential transfer printing of graphene grown on copper foils. TM polarized reflectivity maps of SPPs for a silver surface and the surface coated with monolayer, bilayer, and trilayer graphene are given in Fig. 3(a). Three distinct features of reflectivity curves appear after coating the surface with graphene layers, (1) resonance wavelength shifts to longer wavelength, (2) the spectral width of the resonance curve increases, and (3) excitation efficiency of SPPs changes with increasing number of graphene layer. Fig. 3(b) shows the overlaid reflection spectra at constant angle for silver and gold, respectively. The SP resonance wavelength is obtained from the minima in the reflectivity spectra. With increasing number of graphene layer, the spectral width of the SP resonance increases. This increase in the spectral width of the reflection curve indicates larger optical losses. Each graphene layer introduces additional loss owing to the interband optical absorption of graphene. Fig. 3(c) shows the resonance wavelength and full width at half maximum (FWHM) of the resonance for silver and gold, respectively. The FWHM on bare silver is around 32 nm and then it increases to 80 nm after coating with trilayer graphene. Each layer introduces a red shift in resonance wavelength of around 30 nm for silver and 15 nm for gold. Fig. 3(d) shows the calculated dispersion relations of SPP on silver surface using Drude model (red curve) and frequency dependent dielectric constant[32] (blue curve). The dispersion relation of graphene coated surface is shown with a black line. The inset shows the magnified dispersion relation of silver surface coated with multilayer graphene. The green line is the dispersion relation of light in free space. (The reflectivity maps and dispersion curves for graphene-gold surface are given in supplemental material.[31])

Having the basic characterization of the surface plasmon-polaritons on graphene-metal surface, we would like to demonstrate a plasmon resonance sensor based on graphene-metal surface. The fabricated sensor provides a unique setup to study the adsorption of organic molecules on graphene surface. Understanding the adsorption of organic molecules from aqueous solution on carbon materials has significant importance for wide spectrum of applications such as analysis of drinking water, waste water treatment,

This article is copyrighted as indicated in the article. Reuse of AIP content is subject to the terms at: http://scitation.aip.org/termsconditions. Downloaded to IP: 139.179.2.116 On: Tue, 15 Jul 2014 06:31:48

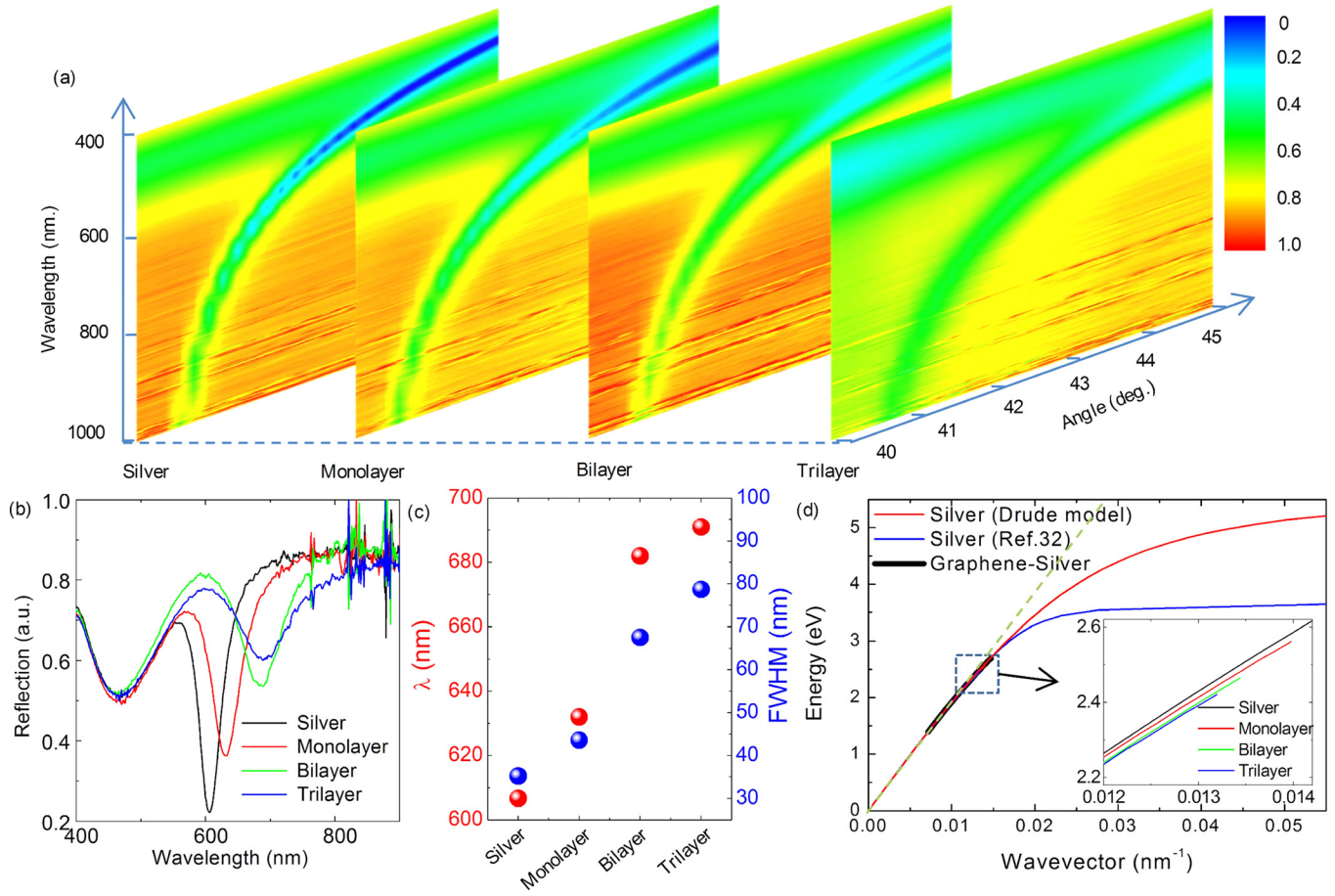


FIG. 3. (a) TM-polarized reflectivity maps of multilayer graphene on a silver surface. (b) Overlaid reflection spectra of multilayer graphene-silver surface at constant angle (42°). (c) The resonance wavelength and the FWHM of SPP on graphene-silver surface as a function of layer number. (d) Calculated dispersion relations of SPP on silver surface using Drude model (red curve) and frequency dependent dielectric constant (blue curve). The dispersion relation of graphene coated surface is shown with black line. The inset shows the magnified dispersion relation of silver surface coated with multilayer graphene. The green line is the dispersion relation of light in free space.

and pharmaceutical industry.[33] Activated carbon is the most commonly used material for these types of applications. Due to the large surface area, graphene based materials could be used for similar applications. The fabricated graphene based surface plasmon sensor is used to elucidate the adsorption of organic molecules on graphene surface. The sensitivity of the sensor decreases due to the lower quality factor of the plasmon resonance. The presence of graphene coating enhances the nonspecific binding of organic molecules due to pi-stacking interactions. We do not expect any specificity; however, the surface can be functionalized for specific binding. We fabricated an elastomeric microfluidic device to control the flow on the graphene coated gold surface. The microfluidic flow chamber allows us to study the adsorption of molecules on graphene surface from an aqueous solution. Binding of molecules on a surface can be modeled with single association-dissociation step. The change of surface concentration of the adsorbent can be described with the following differential equation

$$\frac{dC}{dt} = k_a A(B_0 - C) - k_d C, \tag{2}$$

where C is the surface concentration of the adsorbent, k_a and k_d are the association and dissociation constants, A is the analyte concentration, and B_0 is the surface concentration of binding site. During association and dissociation phases, the solution of the differential equation gives exponential saturation and decay curves, respectively. Fitting the curves provides quantitative kinetic parameters. Using the fabricated SPR sensor, we first examined adsorption of a serum albumin protein (BSA) on graphene surface. The incidence angle was set to 49°, which provides the steepest slope in the reflectivity curve. First, we flowed deionized water (DI water) for 20 min and then introduced 500 nM BSA solution. The real time reflection is shown in Fig. 4. The SPR signal increases as the graphene surface covered by the proteins. After 20 min when the SPR signal becomes saturated, we stopped the flow of BSA solution and washed the chamber with DI water. We recorded the SPR signal for 60 min in order to see desorption of the protein from the graphene surface. We do not observe any significant change in the reflection for 60 min. This observation indicates a very small dissociation rate of BSA on graphene surface. To determine the association constant, we repeated the experiments for three different BSA concentrations. The inset in Fig. 4 shows the inverse of the time constant as a function of analyte concentration. The slope of the curve determines the association (k_a) constant of 2.4×10^{-5} M^{-1} s^{-1}. The intersection provides the dissociation constant (k_d), which is found to be very small indicating that BSA is kinetically stable on graphene surface. The association constant of BSA on graphene

This article is copyrighted as indicated in the article. Reuse of AIP content is subject to the terms at: http://scitation.aip.org/termsconditions. Downloaded to IP: 139.179.2.116 On: Tue, 15 Jul 2014 06:31:48

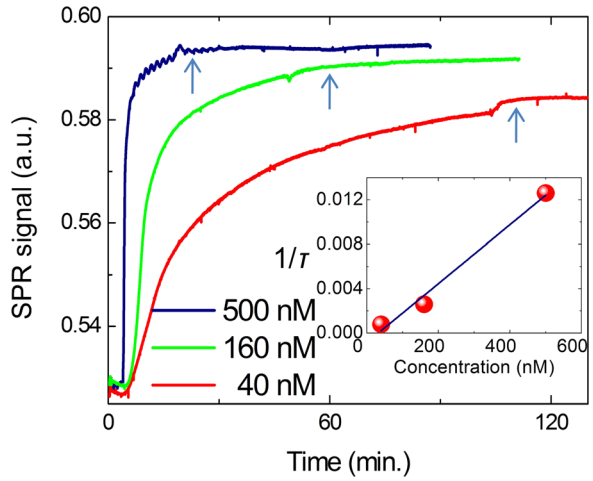


FIG. 4. Overlaid binding interaction plot for BSA for concentration from 40 nM to 500 nM interacting with graphene layer. The inset shows the calculated time constant of the exponential saturation curves. The slope of the curve provides association constant k_a of 2.4×10^{-5} M^{-1} s^{-1}.

layer is three times smaller than anti-BSA coated surface (7.4×10^{-5} M^{-1} s^{-1}).

As a summary, we studied excitation of surface plasmon-polaritons on graphene-metal surface. The metal surface is functionalized by transfer printing of graphene grown by chemical vapor deposition on copper foils. Surface plasmon resonance characteristics of monolayer and multilayer graphene on the metal surface are presented. We were able to obtain the dispersion relation of graphene-metal surface, which reveals the essential feature of the plasmon-polaritons. As an application, we fabricated a surface plasmon resonance sensor integrated with a microfluidic device to study nonspecific physical interaction between graphene layer and proteins. We anticipate that graphene based surface plasmon sensors can be used to analyze adsorption of organic solutes from an aqueous solution on graphitic surface which has wide spectrum of application for environmental protection and pharmaceutical industry.

This work is supported by the Scientific and Technological Research Council of Turkey (TUBİTAK) Grant Nos: 110T304 and 109T259, Marie Curie International Reintegration Grant (IRG) Grant No. 256458 and Turkish Academy of Science (TUBA).

[1]A. K. Geim and K. S. Novoselov, Nature Mater. **6**, 183–191 (2007).
[2]Y. Q. Wu, Y. M. Lin, A. A. Bol, K. A. Jenkins, F. N. Xia, D. B. Farmer, Y. Zhu, and P. Avouris, Nature **472**, 74–78 (2011).
[3]Y. M. Lin, A. Valdes-Garcia, S. J. Han, D. B. Farmer, I. Meric, Y. N. Sun, Y. Q. Wu, C. Dimitrakopoulos, A. Grill, P. Avouris, and K. A. Jenkins, Science **332**, 1294–1297 (2011).
[4]P. Avouris, Nano Lett. **10**, 4285–4294 (2010).
[5]I. Meric, M. Y. Han, A. F. Young, B. Ozyilmaz, P. Kim, and K. L. Shepard, Nat. Nanotechnol. **3**, 654–659 (2008).
[6]A. Reina, X. T. Jia, J. Ho, D. Nezich, H. B. Son, V. Bulovic, M. S. Dresselhaus, and J. Kong, Nano Lett. **9**, 3087–3087 (2009).
[7]C. Kocabas and E. Pince, Appl. Phys. Lett. **97**, 173106 (2010).
[8]J. A. Rogers, Nat. Nanotechnol. **3**, 254–255 (2008).
[9]F. Bonaccorso, Z. Sun, T. Hasan, and A. C. Ferrari, Nat. Photonics **4**, 611–622 (2010).
[10]F. N. Xia and P. Avouris, IEEE Photon. J. **3**, 293–295 (2011).
[11]T. Mueller, F. N. A. Xia, and P. Avouris, Nat. Photonics **4**, 297–301 (2010).
[12]J. M. Lee, J. W. Choung, J. Yi, D. H. Lee, M. Samal, D. K. Yi, C. H. Lee, G. C. Yi, U. Paik, J. A. Rogers, and W. I. Park, Nano Lett. **10**, 2783–2788 (2010).
[13]F. H. L. Koppens, D. E. Chang, and F. J. G. de Abajo, Nano Lett. **11**, 3370–3377 (2011).
[14]M. Jablan, H. Buljan, and M. Soljacic, Phys. Rev. B **80**, 245435 (2009).
[15]S. Y. Shin, N. D. Kim, J. G. Kim, K. S. Kim, D. Y. Noh, K. S. Kim, and J. W. Chung, Appl. Phys. Lett. **99**, 082110 (2011).
[16]L. A. Falkovsky and S. S. Pershoguba, Phys. Rev. B **76**, 153410 (2007).
[17]Z. Fei, G. O. Andreev, W. Z. Bao, L. F. M. Zhang, A. S. McLeod, C. Wang, M. K. Stewart, Z. Zhao, G. Dominguez, M. Thiemens, M. M. Fogler, M. J. Tauber, A. H. Castro-Neto, C. N. Lau, F. Keilmann, and D. N. Basov, Nano Lett. **11**, 4701–4705 (2011).
[18]X. Zhang, M. Liu, X. B. Yin, E. Ulin-Avila, B. S. Geng, T. Zentgraf, L. Ju, and F. Wang, Nature **474**, 64–67 (2011).
[19]F. Wang, C. F. Chen, C. H. Park, B. W. Boudouris, J. Horng, B. S. Geng, C. Girit, A. Zettl, M. F. Crommie, R. A. Segalman, and S. G. Louie, Nature **471**, 617–620 (2011).
[20]F. Wang, Y. B. Zhang, C. S. Tian, C. Girit, A. Zettl, M. Crommie, and Y. R. Shen, Science **320**, 206–209 (2008).
[21]S. H. Choi, Y. L. Kim, and K. M. Byun, Opt. Express **19**, 458–466 (2011).
[22]L. Wu, H. S. Chu, W. S. Koh, and E. P. Li, Opt. Express **18**, 14395–14400 (2010).
[23]N. Papasimakis, Z. Q. Luo, Z. X. Shen, F. De Angelis, E. Di Fabrizio, A. E. Nikolaenko, and N. I. Zheludev, Opt. Express **18**, 8353–8359 (2010).
[24]S. F. Shi, X. D. Xu, D. C. Ralph, and P. L. McEuen, Nano Lett. **11**, 1814–1818 (2011).
[25]E. Cubukcu, F. Degirmenci, C. Kocabas, M. A. Zimmler, J. A. Rogers, and F. Capasso, Proc. Natl. Acad. Sci. U.S.A. **106**, 2495–2499 (2009).
[26]E. Cubukcu, E. A. Kort, K. B. Crozier, and F. Capasso, Appl. Phys. Lett. **89**, 093120 (2006).
[27]G. B. Sigal, C. Bamdad, A. Barberis, J. Strominger, and G. M. Whitesides, Anal. Chem. **68**, 490–497 (1996).
[28]S. S. Chen, L. Brown, M. Levendorf, W. W. Cai, S. Y. Ju, J. Edgeworth, X. S. Li, C. W. Magnuson, A. Velamakanni, R. D. Piner, J. Y. Kang, J. Park, and R. S. Ruoff, ACS Nano **5**, 1321–1327 (2011).
[29]L. Colombo, X. S. Li, W. W. Cai, J. H. An, S. Kim, J. Nah, D. X. Yang, R. Piner, A. Velamakanni, I. Jung, E. Tutuc, S. K. Banerjee, and R. S. Ruoff, Science **324**, 1312–1314 (2009).
[30]T. Oznuluer, E. Pince, E. O. Polat, O. Balci, O. Salihoglu, and C. Kocabas, Appl. Phys. Lett. **98**, 183101 (2011).
[31]See supplementary material at http://dx.doi.org/10.1063/1.4721453 for Raman spectra of multilayer graphene (Fig. S1), SPR wavelength as a function of incidence angle for silver-graphene and gold-graphene surfaces (Fig. S2), reflectivity maps and dispersion curves for gold-graphene surface (Fig. S3).
[32]E. D. Palik, *Handbook of Optical Constants of Solids* (Academic, Boston, 1985).
[33]C. Moreno-Castilla, Carbon **42**, 83–94 (2004).

This article is copyrighted as indicated in the article. Reuse of AIP content is subject to the terms at: http://scitation.aip.org/termsconditions. Downloaded to IP: 139.179.2.116 On: Tue, 15 Jul 2014 06:31:48